Synthesis and Characterization of the Tetranuclear Ru^{II} Complex $[RuCl(\mu\text{-}Cl)(P(OMe)_3)_2(\mu,\eta^1,\eta^2\text{-}S_2)Ru(P(OMe)_3)(\mu\text{-}P(OMe)_3\text{-}P,O)]_2$ Containing a *trans*-$Ru^{II}SSRu^{II}$ Core

Tetsuya Koyama,[†] Yoshihiro Koide,[‡] and Kazuko Matsumoto*[,†,‡]

Department of Chemistry and Advanced Research Center for Science and Engineering, School of Science and Engineering, Waseda University, Tokyo 169-8555, and Japan Science and Technology Corporation, Saitama 332-0012, Japan

Received October 26, 1998

Introduction

We have extensively studied the coordination chemistry of the Cl-bridged dinuclear $Ru^{II}Ru^{III}$, $Ru^{III}Ru^{III}$, and $Ru^{II}Ru^{II}$ complexes.[1] One of our objectives is to coordinate external dinitrogen in the μ-N_2 mode between the two ruthenium centers and subsequently reduce the nitrogen atom to NH, NH_2, or NH_3. Previously, we attempted to remove the bridging chlorides in the dinuclear Ru complexes under a nitrogen atmosphere in expectation of achieving μ-N_2 coordination. When the Ru^{III}-Ru^{III} complex $[RuCl(P(OMe)_3)_2]_2(\mu\text{-}Cl)_2(\mu\text{-}S_2)$ (**1**) was oxidized by 2 equiv of $AgCF_3SO_3$ in CH_3CN at room temperature, Ag^+ extracted the terminal chlorides instead of the bridging chlorides to yield $\{[Ru(CH_3CN)(P(OMe)_3)_2]_2(\mu\text{-}Cl)_2(\mu\text{-}S_2)\}^{2+}$ (**2**) (Scheme 1).[1b]

Removal of the bridging chlorides in complex **2** by metallic magnesium in CH_3OH resulted in the formation of the Ru^{II}_2-Ru^{III}_2 mixed-valent tetranuclear complex, $[Ru(P(OMe)_3)_2]_4(\mu\text{-}H)_2(\mu\text{-}S)_2(\mu_4\text{-}S)_2$ (**3**).[2] When the oxidation of **1** by $AgCF_3SO_3$ was conducted at 50 °C, not only the terminal chlorides but also the bridging chlorides were removed in a single reaction to yield the $Ru^{II}Ru^{III}$ mixed-valent dinuclear complex, $\{[Ru(CH_3CN)_3(P(OMe)_3)_2]_2(\mu\text{-}S_2)\}^{3+}$ (**4**).[1i] In this reaction, complex **4** must be preceded by complex **2**, which loses the two bridging chlorides under elevated temperature (Scheme 1). Reduction of a THF solution of **1** by metallic sodium at room temperature resulted in elimination of one of the two bridging chlorides to yield the novel tetranuclear Ru^{II} complex, $[Na_2Ru_4(P(OMe)_3)_4(\mu\text{-}Cl)_4(\mu_4\text{-}Cl)_2(\mu,\eta^2\text{-}S_2)_2(\mu\text{-}P(OMe)_3\text{-}P,O)_4]\cdot$THF (**5**·THF).[3] From

Scheme 1

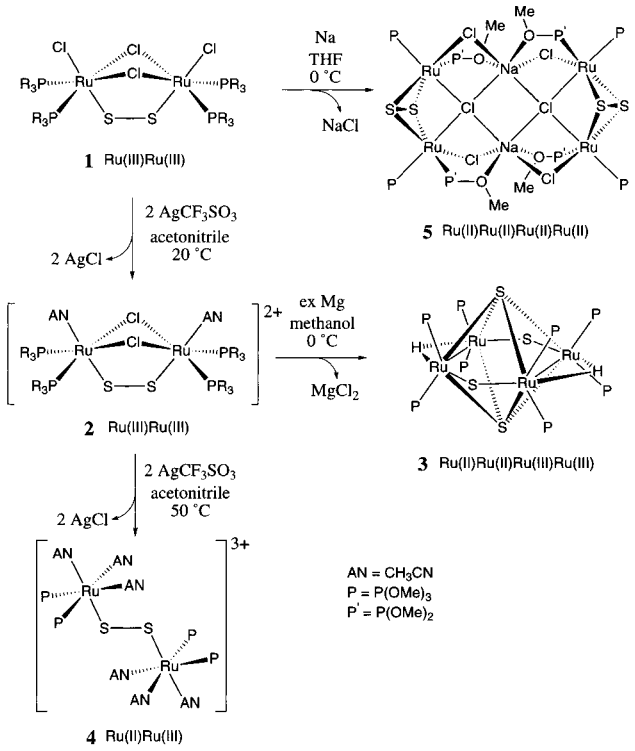

a series of experiments it is clear that **1** generates a variety of products under different oxidation/reduction conditions.

In this note, we report a reexamination of the reduction conditions of complex **1** and employ sodium amalgam as a reductant that allows quantitative reduction of Ru^{III} to Ru^{II}. The reduction in THF leads to complete removal of the bridging chlorides to yield the tetranuclear Ru^{II} complex, $[RuCl(\mu\text{-}Cl)(P(OMe)_3)_2(\mu,\eta^1,\eta^2\text{-}S_2)Ru(P(OMe)_3)(\mu\text{-}P(OMe)_3\text{-}P,O)]_2$ (**6**), although it exhibits no affinity to dinitrogen. Complex **6** has, however, a unique structure that consists of two *trans*-$Ru^{II}SSRu^{II}$ cores aligned parallel to each other. The result of the X-ray study of **6** is presented along with a discussion of the proposed reaction pathways clarified by $^{31}P\{^1H\}$ NMR spectroscopy.

Experimental Section

General Methods. All synthetic procedures were performed under purified nitrogen using standard Schlenk techniques or in a nitrogen atmosphere glovebox unless otherwise mentioned. Commercially available anhydrous solvents were used without further purification. Solution $^{31}P\{^1H\}$ NMR spectra were obtained on a JEOL EX-270WB spectrometer using $CDCl_3$, and the chemical shifts were recorded in reference to a $P(OMe)_3/(CD_3)_2CO$ external standard set at 140 ppm. IR spectra were recorded in KBr matrix.

Synthesis of the Title Complex. A THF (20 mL) suspension of **1**[1j] (0.20 g, 0.22 mmol) was placed in an autoclave, which consists of a two-piece acrylic resin jacket equipped with a pressure gauge and a fitting 100 mL glass vessel. The autoclave was then sonicated for ca. 30 min to the point where no visibly large grain of **1** was left. To the vessel was added 0.35 g (0.44 mmol) of sodium amalgam (2.9%),[4] and the vessel was filled with N_2 gas at 15 atm. The autoclave was then kept at −37 °C, and vigorously stirred for 1−2 weeks until the reaction solution became a light-brown homogeneous solution. Any

* Address all correspondence to this author at Department of Chemistry, Waseda University, Tokyo 169-8555, Japan.
† Waseda University.
‡ Japan Science and Technology Corporation.

(1) (a) *Transition Metal Sulfur Chemistry: Biological and Industrial Significance*; Stiefel, E., Matsumoto, K., Eds.; ACS Symposium Series 653; American Chemical Society: Washington, DC, 1996; Chapter 15. (b) Matsumoto, K.; Matsumoto, T.; Kawano, M.; Ohnuki, H.; Shichi, Y.; Nishide, T.; Sato, T. *J. Am. Chem. Soc.* **1996**, *118*, 3597. (c) Matsumoto, K.; Uemura, H.; Kawano, M. *Chem. Lett.* **1994**, 1215. (d) Kawano, M.; Uemura, H.; Watanabe, T.; Matsumoto, K. *J. Am. Chem. Soc.* **1993**, *115*, 2068. (e) Kawano, M.; Hoshino, C.; Matsumoto, K. *Inorg. Chem.* **1992**, *31*, 5158. (f) Uemura, H.; Kawano, M.; Watanabe, T.; Matsumoto, T.; Matsumoto, K. *Inorg. Chem.* **1992**, *31*, 5137. (g) Kato, M.; Kawano, M.; Taniguchi, H.; Funaki, M.; Moriyama, H.; Sato, T.; Matsumoto, K. *Inorg. Chem.* **1992**, *31*, 26. (h) Kawano, M.; Watanabe, T.; Matsumoto, K. *Chem. Lett.* **1992**, 2389. (i) Matsumoto, T.; Matsumoto, K. *Chem. Lett.* **1992**, 1539. (j) Matsumoto, T.; Matsumoto, K. *Chem. Lett.* **1992**, 559. (k) Matsumoto, T.; Matsumoto, K.; Sato, T. *Inorg. Chim. Acta* **1992**, *202*, 31.
(2) Matsumoto, K.; Ohnuki, H.; Kawano, M. *Inorg. Chem.* **1995**, *34*, 3838.
(3) Matsumoto, K.; Sano, Y. *Inorg. Chem.* **1997**, *36*, 4405.
(4) Booth, H. S. ed. *Inorganic Synthesis*: McGraw-Hill: New York, 1939; p 10.

10.1021/ic9812508 CCC: $18.00
Published on Web 06/02/1999

Table 1. Summary of Crystal Data for **6**·THF

formula	$C_{28}H_{80}O_{25}P_8S_4Cl_4Ru_4$	Z	2
fw	1739.05	d_{calcd}, g cm^{-3}	1.953
cryst syst	monoclinic	abs coeff (μ), cm^{-1}	16.14
space group	$P2_1/a$ (No. 14)	abs corr	DIFABS[d]
a, Å	13.582(2)	radiation (λ), Å	Mo Kα (0.710 69)
b, Å	15.813(2)	R[a]	0.043
c, Å	14.753(1)	R_w[b]	0.047
β, deg	111.008(8)	GOF[c]	2.00
V, Å^3	2957.8(6)	T, °C	0,0

[a] $R = \sum(|F_o| - |F_c|)/\sum|F_o|$. [b] $R_w = [\sum w (|F_o| - |F_c|)^2/\sum w|F_o|^2]^{1/2}$, $w = 1/\sigma(F_o)^2$. [c] GOF $= [\sum w(|F_o| - |F_c|)^2/\sum(N_{reflns} - N_{params})]^{1/2}$. [d] DIFABS: An empirical absorption correction program. See ref 6.

insolubility (mostly NaCl and Hg) was removed by centrifugation followed by filtration. The filtrate was layered with ca. 30 mL of hexane at 0 °C to yield yellow X-ray quality crystals of **6**·THF.[5] ^{31}P{^{1}H} NMR (δ ppm): 175 [d, $J_{p-p} = 73.0$ Hz, $P(\mu,\eta^2$-OMe)(OMe)$_2$], 157 [d, $J_{p-p} = 73.0$ Hz, P(OMe$_3$)$_3$], 144 [d, $J_{p-p} = 94.4$ Hz, RuP(OMe)$_3$P(OMe)$_3$], 140 [d, $J_{p-p} = 94.4$ Hz, RuP(OMe)$_3P$(OMe)$_3$]. The sample subjected to elemental analysis was a mixture of **6** and **6**·THF, and the calculation value agreed with the experimental value when 0.9 molecule of THF was included. Anal. Calcd for $C_{27.6}H_{79.2}O_{24.9}P_8S_4Cl_4Ru_4$: C, 19.14; H, 4.61. Found: C, 19.16; H, 4.41. Yield: 26%.

Collection and Reduction of X-ray Data. A crystal of **6**·THF ($0.5 \times 0.2 \times 0.2$ mm^3) was subjected to single-crystal X-ray diffraction analysis. Because the crystal decays slowly at room temperature, X-ray measurement was performed at 0 °C. Unit cell parameters were obtained from a least-squares fit of 24 reflections in the range $20.5° < 2\theta < 24.5°$ measured on a Rigaku AFC-7R four-circle diffractometer using graphite-monochromated Mo Kα radiation (0.710 69 Å). The Lorentz−polarization and absorption[6] corrections were made to the collected data. The crystal data are give in Table 1, and the details of the data collection are in Table S1 (Supporting Information).

Solution and Refinement of the Structure. The structure of **6**·THF was solved by a direct method and subsequent Fourier techniques. All of the non-hydrogen atoms in the complex were located and were refined anisotropically by a full-matrix least-squares method. All calculations were performed using SHELXS 86. The final atomic positions and thermal parameters for **6**·THF are listed in Table S2 (Supporting Information). The anisotropic thermal parameters are deposited in Table S3 (Supporting Information).

Results and Discussion

Synthesis and Properties of Complex 6. The yield of complex **6** depends strongly on the reaction temperature. In an attempted synthesis at room temperature, the reaction solution turned brown within 1 week, and no product was obtained analytically pure. In a successful synthesis, on the other hand, the reaction vessel was kept at −37 °C throughout the reaction, in which the solution gradually turned light brown over 2 weeks. The proposed reaction pathway is shown in Scheme 2.

The initial step of the reaction is the reduction of the two Ru^{III} centers in **1** to Ru^{II} by 2 equiv of metallic sodium, concomitant with extraction of the bridging chloride by Na$^+$ as NaCl to yield an intermediate **I**. Previously we reported that Ag$^+$ extracts exclusively the terminal chloride at room temperature and the bridging chloride remains intact.[1b] On the other hand, Na$^+$ and Mg^{2+} preferentially extract the bridging chloride.[2,3] The reduction of Ru^{III} to Ru^{II} must be followed by rotation about the S−S bond that generates a trans configuration which is thermodynamically favorable. Simultaneously, solvent molecules coordinate to the Ru^{II} centers to fill the coordination vacancies (**I**). The resulting dinuclear Ru^{II} species is considered to exist as an individual molecule only in the solvent, and two molecules of **I** merge and crystallize as complex **6**. The ^{31}P{^{1}H} NMR spectrum of the reaction solution shows that the resonance corresponding to **6** does not appear at any point. Indeed, the isolated crystals of **6** are hardly soluble in THF.

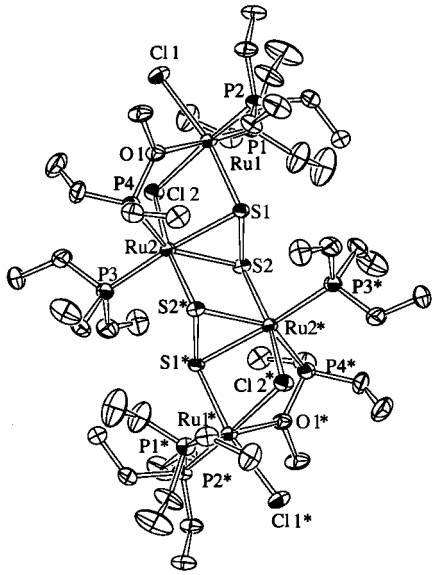

Figure 1. ORTEP diagram of [RuCl(μ-Cl)(P(OMe)$_3$)$_2$(μ,η^1,η^2-S$_2$)Ru(P(OMe)$_3$)(μ-P(OMe)$_3$-*P*,*O*)]$_2$ (**6**·THF) showing 50% probability thermal ellipsoids for all non-hydrogen atoms.

Scheme 2

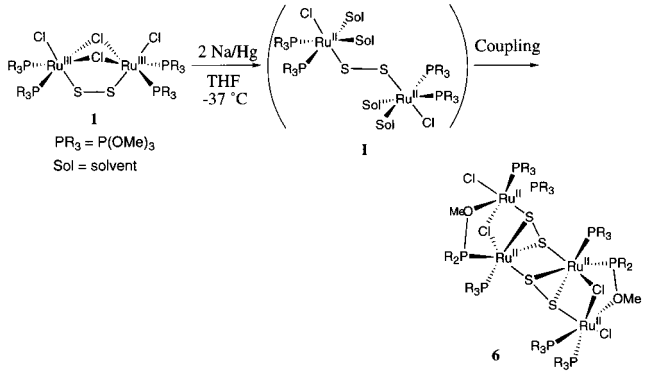

Structure of 6. The monosolvated **6**·THF was subjected to X-ray diffraction. The ORTEP diagram is shown in Figure 1, and the selected bond distances and angles are listed in Table 2.

The two halves of **6**·THF are related through a true crystallographic inversion center that sits at the center of the rhombic Ru$_2$S$_2$ core. The structure can be viewed as two *trans*-Ru^{II}SSRu^{II} cores[1i] aligned parallel to each other and linked through newly generated μ,η^1,η^2-S$_2$, μ-Cl, and μ-P(OMe)$_3$-*P*,*O* groups. The μ-Cl and the μ-P(OMe)$_3$-*P*,*O* groups are doubly bridging the two coordinatively nonequivalent Ru^{II} centers, which have distorted octahedral coordination environments. Such a *trans*-RuSSRu configuration is ubiquitous, including contributions from this laboratory such as complex **4**[1i] and {[Ru$_2$(CH$_3$CN)$_3$(P(OMe)$_3$)$_4$](μ-S$_2$CH$_2$COCH$_3$)}(CF$_3$SO$_3$)$_3$·0.5(CH$_3$)$_2$O (**7**),[7] but a complex with the *trans*-Ru^{II}SSRu^{II} core is rare.[1b] The RuSSRu core lies almost in a plane with a dihedral angle of 6.7°. The Ru(2)−S(1) and Ru(2)−S(2) distances (2.403(2) and 2.478(3) Å, respectively) are comparable to the Ru^{II}−μ,η^2-S$_2^{2-}$ distances

(5) Complex **6** crystallizes in two forms, with and without a solvent molecule.

(6) Walker, N.; Stuart, D. *Acta Crystallogr., Sect. A* **1983**, *A39*, 158.

(7) Matsumoto, K.; Uemura, H.; Kawano, M. *Inorg. Chem.* **1995**, *34*, 658.

Table 2. Selected Bond Distances (Å) and Angles (deg) for **6**·THF[a,b]

Bond Distances			
Ru(1)−Cl(1)	2.428(2)	Ru(1)−Cl(2)	2.478(2)
Ru(1)−S(1)	2.332(2)	Ru(1)−P(1)	2.167(3)
Ru(1)−P(2)	2.206(3)	Ru(1)−O(1)	2.382(6)
Ru(2)−Cl(2)	2.446(2)	Ru(2)−S(1)	2.403(2)
Ru(2)−S(2)	2.478(3)	Ru(2)−S(2*)	2.368(2)
Ru(2)−P(3)	2.247(3)	Ru(2)−P(4)	2.205(3)
S(1)−S(2)	2.102(3)	P(4)−O(1)	1.642(6)

Bond Angles			
Cl(1)−Ru(1)−Cl(2)	89.46(9)	Cl(1)−Ru(1)−S(1)	166.88(10)
Cl(1)−Ru(1)−P(1)	92.59(10)	Cl(1)−Ru(1)−P(2)	95.45(10)
Cl(1)−Ru(1)−O(1)	83.7(2)	Cl(2)−Ru(1)−S(1)	84.06(8)
Cl(2)−Ru(1)−P(1)	94.20(10)	Cl(2)−Ru(1)−P(2)	171.27(9)
Cl(2)−Ru(1)−O(1)	83.0(2)	S(1)−Ru(1)−P(1)	99.23(9)
S(1)−Ru(1)−P(2)	89.66(9)	S(1)−Ru(1)−O(1)	84.2(2)
P(1)−Ru(1)−P(2)	92.8(1)	P(1)−Ru(1)−O(1)	175.3(2)
P(2)−Ru(1)−O(1)	90.3(2)	Cl(2)−Ru(2)−S(1)	83.29(8)
Cl(2)−Ru(2)−S(2)	86.14(8)	Cl(2)−Ru(2)−S(2)	167.78(9)
Cl(2)−Ru(2)−P(3)	91.78(9)	Cl(2)−Ru(2)−P(4)	89.12(9)
S(1)−Ru(2)−S(2)	50.99(8)	S(1)−Ru(2)−S(2)	89.33(8)
S(1)−Ru(2)−P(3)	167.72(9)	S(1)−Ru(2)−P(4)	95.18(9)
S(2)−Ru(2)−S(2)	81.64(8)	S(2)−Ru(2)−P(3)	117.62(9)
S(2)−Ru(2)−P(4)	146.16(9)	S(2)−Ru(2)−P(3)	93.49(9)
S(2)−Ru(2)−P(4)	101.28(9)	P(3)−Ru(2)−P(4)	96.0(1)

[a] See Figure 1 for the atom-labeling scheme. [b] Numbers in parentheses are estimated standard deviations for the last significant digit.

(2.334(5)−2.527(5) Å) found in **5**·THF.[3] The two Ru−S distances in the *trans*-RuSSRu (Ru(1)−S(1) = 2.332(2) Å, Ru(2)−S(2*) = 2.368(2) Å) are consistent with those found in **4** (2.322(2) Å) and in **7** (2.339(5) and 2.380(5) Å). It is noteworthy that the Ru−S distance in the *trans*-RuSSRu are longer than the typical values found in its cis analogue and are little affected by the metal oxidation state. The Ru(1)−P (phosphite) distances (2.167(3) and 2.206(3) Å), the Ru(2)−P (μ-phosphite) distance (2.205(3) Å), and the Ru(2)−P (phosphite) distance (2.247(3) Å) in **6**·THF are also comparable to those in **5** (2.186(6)−2.204(6) Å). The S(1)−S(2) distance (2.102(3) Å) in the μ-S_2^{2-} or μ,η^2-S_2^{2-} ligands of **6**·THF is longer than any of previously reported values,[8] reflecting that the S−S single bond order is reduced under μ,η^2-mode coordination. Upon coordination of $O_{methoxy}$ in $P(OMe)_3$ to Ru, the P(4)−O(1) distance (1.642(6) Å) becomes slightly longer than that in the noncoordinated methoxy groups (1.590(7) and 1.602(7) Å). The difference is reflected in ν(P−O), which shows a lower frequency shift from 728 cm^{-1} (noncoordinated) to 692 cm^{-1} (coordinated).

^{31}P{^{1}H} NMR Studies. The single crystals of **6**·THF were dissolved in $CDCl_3$, and the ^{31}P{^{1}H} NMR spectrum was observed (Figure 2).

Despite dissolution of single crystals, the spectrum exhibits two sets of four doublets, indicating the coexistence of two

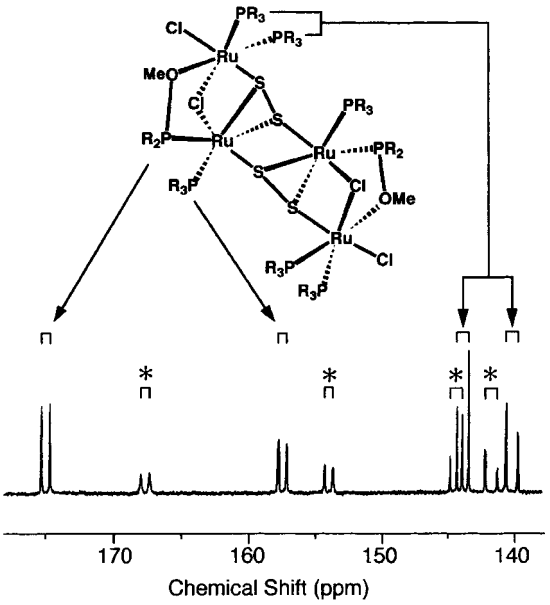

Figure 2. ^{31}P {^{1}H} NMR spectrum of **6** in $CDCl_3$.

structures with different modes of $P(OMe)_3$ coordination. Among those two sets, the set of dominant peaks (175, 157, 144, and 140 ppm) was assigned as **6**. Generally, ^{31}P NMR chemical shifts of $Ru^{II}(P(OMe)_3)_n$ appear at ca. 135 ppm or lower field, and those of $Ru^{III}(P(OMe)_3)_n$ at the vicinity of 123 ppm.[9] Two resonances at 144 and 140 ppm in complex **6** correspond to the two $P(OMe)_3$ ligands, which coordinated cis to $Ru^{II}(1)$. The resonances at 175 and 157 ppm are assigned as two unique phosphite ligands on the $Ru^{II}(2)$, μ-$P(OMe)_3$-*P*,*O* and $P(OMe)_3$, respectively. Of the second set of peaks (168, 154, 144.3, and 141.8 ppm: shown with asterisks), resonances at 144.3 and 141.8 ppm are readily assigned as the two $P(OMe)_3$ ligands cis to each other. However, the resonances at 168 and 154 ppm exhibit substantial upfield shifts from the corresponding resonances observed in complex **6** (175 and 157 ppm, respectively). The magnitude of the shift is larger for μ-$P(OMe)_3$-*P*,*O*, presumably because the Ru−O (phosphite) bond (2.382(6) Å), which is considerably longer than the sum of covalent radii (2.08 Å), undergoes cleavage upon dissolution. Concomitantly, the coordination vacancy on the ruthenium will be filled by $CDCl_3$.

Acknowledgment. We are grateful for the financial support by CREST (Core Research for Evolutional Science and Technology) of the Japan Science and Technology Corporation (JST). We gratefully acknowledge the assistance of Mr. Ryosuke Somazawa with X-ray crystallographic data processing.

Supporting Information Available: X-ray crystallographic data for **6**·THF, including tables of crystal and intensity collection data, positional and thermal parameters, and interatomic distances and angles. This material is available free of charge via the Internet at http://pubs.acs.org.

IC9812508

(8) (a) Sellmann, D.; Lechner, P.; Knoch, F.; Moll, M. *J. Am. Chem. Soc.* **1992**, *114*, 922. (b) Mizobe, Y.; Hosomizu, M.; Kawabata, J.; Hidai, M. *J. Chem. Soc., Chem. Commun.* **1991**, 1226. (c) Amarasekera, J.; Rauchfuss, T. B.; Wilson, S. R. *Inorg. Chem.* **1987**, *26*, 3328. (d) Rauchfuss, T. B.; Rodgers, D. P. S.; Wilson, S. R. *J. Am. Chem. Soc.* **1986**, *108*, 3114. (e) Kim, S.; Otterbein, E. S.; Rava, R. P.; Isied, S. S.; Filippo, J. S., Jr.; Waszczyak, J. V. *J. Am. Chem. Soc.* **1983**, *105*, 336. (f) Müller, A.; Jagermann, W.; Enemark, J. H. *Coord. Chem. Rev.* **1982**, *46*, 245. (g) Elder, R. C.; Trkula, M. *Inorg. Chem.* **1977**, *16*, 1048.

(9) Koyama, T.; Koide, Y.; Matsumoto, K. Manuscript in preparation.